arXiv:1008.1152v2 [astro-ph.CO] 7 Oct 2010

Non-Gaussianity with Lagrange Multiplier Field in the Curvaton Scenario

Chao-Jun Feng[1, *] and Xin-Zhou Li[1, †]
[1] *Shanghai United Center for Astrophysics (SUCA),*
Shanghai Normal University, 100 Guilin Road, Shanghai 200234, P.R.China

In this paper, we will use $\delta\mathcal{N}$-formalism to calculate the primordial curvature perturbation for the curvaton model with a Lagrange multiplier field. We calculate the non-linearity parameters f_{NL} and g_{NL} in the sudden-decay approximation in this kind of model, and we find that one could get a large non-Gaussinity even if the curvaton dominates the total energy density before it decays, and this property will make the curvaton model much richer. We also calculate the probability density function of the primordial curvature perturbation in the sudden-decay approximation, as well as some moments of it.

PACS numbers: 98.80.Cq

I. INTRODUCTION

Inflation has been remarkably successful in explaining the properties of the universe and the origin of the primordial perturbation [1], which is thought of as the seed of the large scale structures. So far, there still a lot of discussions and works on inflation, such as [2]. A single-field inflation predicts a nearly Gaussian distribution of the primordial power spectrum [3]. On the other hand, multi-field models of inflation can lead to a large deviation from the Gaussian distribution, which may be observed in the future observations [4]. In fact, the multi-field models generate the non-Gaussianity due to the non-trivial classical dynamics on superhorizon scales. Since the gravitational dynamics could introduce significant non-linearities that would contribute to the final non-Gaussianity in the large scale of CMB anisotropies, the CMB non-Gaussianity opens a window to probe the physics of the early universe.

There are many mechanisms to generate a large local-type non-Gaussinities, and one of them is the curvaton scenario [5]. In this kind of model, there would be another, weakly coupled, light inhomogeneous scalar field called curvaton, whose energy density could be neglected during inflation, while the early Universe is dominated by inflaton. After the end of inflation, the energy of inflaton converted into radiations and the Hubble parameters decreases. During the evolution of the curvaton, its energy density goes like $\propto a^{-3}$, which increases with respect to that of radiations $\propto a^{-4}$. Therefore, the curvaton can dominate the energy density of the Universe later. When the Hubble parameter becomes the same order of the curvation decay rate, the energy of the curvaton would be converted into radiations. Finally, the curvation is supposed to completely decay into thermalized radiations before primordial nucleosynthesis, in the meanwhile, the perturbations of the curvaton become the final adiabatic curvature perturbations that seed the matter and radiation density fluctuations observed in the Universe. This kind of non-Gaussianity can be described by some non-linearity parameters f_{NL}, g_{NL}, etc. defined below. For recent progress on the curvaton model, see Ref. [6][7][8].

At first, we expand the curvature perturbation as

$$\zeta(t,\mathbf{x}) = \zeta_1(t,\mathbf{x}) + \sum_{n=2}^{\infty}\frac{1}{n!}\zeta_n(t,\mathbf{x})\,, \tag{1}$$

where the probability density function (pdf) of the first order term ζ_1 is Gaussian, while the higher order terms give rise to a non-Gasussian pdf of the full ζ. As usual, the non-linearity parameters f_{NL} and g_{NL} are defined by

$$\zeta = \zeta_1 + \frac{3}{5}f_{NL}\zeta_1^2 + \frac{9}{25}g_{NL}\zeta_1^3 + \mathcal{O}(\zeta_1^4)\,, \tag{2}$$

or, equivlently

$$f_{NL} = \frac{5\zeta_2}{6\zeta_1^2}\,, \quad g_{NL} = \frac{25\zeta_3}{54\zeta_1^3}\,, \tag{3}$$

---

[*] Electronic address: fengcj@shnu.edu.cn
[†] Electronic address: kychz@shnu.edu.cn

where the numerical factors arise in order to be consistent with the Bardeen potential on large scales. The upper bound from the WMAP 3yr data [9] is $|f_{NL}| < 114$, the bound from WMAP 5yr data [10] is $-9 < f_{NL} < 111$ at 2σ level and the constraint from WMAP 7yr data [11] is $f_{NL} = 32 \pm 21$ at 1σ level. The correlation functions of Fourier transformation of ζ are used to define the primordial power spectrum, bispectrum and trispectrum as

$$\begin{aligned}
\langle\zeta(\mathbf{k_1})\zeta(\mathbf{k_2})\rangle &= (2\pi)^3\mathcal{P}_\zeta(k_1)\delta^3\Big(\sum_{n=1}^{2}\mathbf{k}_n\Big)\,, && (4)\\
\langle\zeta(\mathbf{k_1})\zeta(\mathbf{k_2})\zeta(\mathbf{k_3})\rangle &= (2\pi)^3\mathcal{B}_\zeta(\mathbf{k}_1,\mathbf{k}_2)\delta^3\Big(\sum_{n=1}^{3}\mathbf{k}_n\Big)\,, && (5)\\
\langle\zeta(\mathbf{k_1})\zeta(\mathbf{k_2})\zeta(\mathbf{k_3})\zeta(\mathbf{k_4})\rangle &= (2\pi)^3\mathcal{T}_\zeta(\mathbf{k}_1,\mathbf{k}_2,\mathbf{k}_3)\delta^3\Big(\sum_{n=1}^{4}\mathbf{k}_n\Big)\,. && (6)
\end{aligned}$$

Thus, we have

$$\begin{aligned}
\mathcal{B}_\zeta(\mathbf{k}_1,\mathbf{k}_2) &= \frac{6}{5}f_{NL}\Big[\mathcal{P}_\zeta(k_1)\mathcal{P}_\zeta(k_2)+2\text{perms}\Big]\,, && (7)\\
\mathcal{T}_\zeta(\mathbf{k}_1,\mathbf{k}_2,\mathbf{k}_3) &= \frac{18}{25}f_{NL}^2\Big[\mathcal{P}_\zeta(k_1)\mathcal{P}_\zeta(k_2)\mathcal{P}_\zeta(|\mathbf{k}_1-\mathbf{k}_2|)+23\text{perms}\Big]\\
&+\frac{54}{25}g_{NL}\Big[\mathcal{P}_\zeta(k_1)\mathcal{P}_\zeta(k_2)\mathcal{P}_\zeta(k_3)+3\text{perms}\Big]\,. && (8)
\end{aligned}$$

In this paper, these non-linearity parameters will be calculated in the curvaton scenario with a Lagrange multiplier field, which is described by the following action [12]

$$S=\int d^4x\sqrt{-g}\Big[K(\varphi,X)+\lambda\Big(X-V(\varphi)\Big)\Big]\,, \tag{9}$$

where the field λ is a "Lagrange multiplier" without a kinetic term and the scalar field φ could be a curvaton. Here,

$$X\equiv\frac{1}{2}g^{\mu\nu}\nabla_\mu\varphi\nabla_\nu\varphi\,, \tag{10}$$

is a standard kinetic term for the field φ, $K(\varphi,X)$ is arbitrary function of φ and X, and $V(\varphi)$ is an arbitrary function of the scalar field φ. The equations of motion for λ and φ are given by

$$\begin{aligned}
X-V(\varphi) &= 0\,, && (11)\\
K_\varphi-\nabla_\mu(K_X\nabla^\mu\varphi)-\lambda V_\varphi-\nabla_\mu(\lambda\nabla^\mu\varphi) &= 0\,. && (12)
\end{aligned}$$

Here and after we denote the partial derivatives by subscripts. And the energy-momentum tensor is

$$T_{\mu\nu}=(K_X+\lambda)\nabla_\mu\varphi\nabla_\nu\varphi-Kg_{\mu\nu}\,. \tag{13}$$

In the spatially flat FRW universe with the metric $ds^2=dt^2-a^2(t)dx^2$, we consider the homogeneous Lagrange multiplier field so that Eqs. (11) and (12) reduce to

$$\begin{aligned}
\dot\varphi^2-2V(\varphi) &= 0\,, && (14)\\
\frac{K_\varphi}{\sqrt{2V}}-\frac{V_\varphi}{\sqrt{2V}}\Big(2VK_{XX}+K_X+2\lambda\Big)-\sqrt{2V}K_{X\varphi}-3H(K_X+\lambda)-\dot\lambda &= 0\,. && (15)
\end{aligned}$$

And also, the energy density and pressure are given by

$$\begin{aligned}
\rho(\lambda,\varphi) &= 2V(\varphi)(K_X+\lambda)-K\,, && (16)\\
p(\varphi) &= K\big(\varphi,V(\varphi)\big)\,. && (17)
\end{aligned}$$

In this paper, we will consider two interesting cases that studied in [12]. The first case is $K_\varphi=0$ and $V=$ const., in which case, the energy-momentum corresponds to a mixture of a cosmological constant and pressureless dust, so we call this model the $L-\lambda\varphi$ model. From Eqs. (14) and (15), we get

$$\dot\varphi=\sqrt{2V}\,,\quad \dot\lambda+3H(K_X+\lambda)=0\,, \tag{18}$$

with solution

$$\varphi = \sqrt{2V}t\,, \quad \lambda = \frac{\rho_0}{2Va^3} - K_X\,,, \tag{19}$$

where ρ_0 is an integration constant. Thus, the energy density and pressure are given by

$$\rho = \frac{\rho_0}{a^3} - p\,, \quad p = \text{const}\,. \tag{20}$$

The other case is $K = 0$ with arbitrary V, and in this model the energy density evolves exactly the same as dust or matter, so we call this model $D - \lambda\varphi$ model. The equations of motion for this model are

$$\dot\varphi = \sqrt{2V(\varphi)}\,, \quad \ddot\varphi + 3H\dot\varphi + V_\varphi + \lambda^{-1}\dot\lambda\dot\varphi = 0\,, \tag{21}$$

and by using the relation $\ddot\varphi = 2V(\varphi)$, we get the solution

$$\lambda = \frac{\rho_0}{a^3\dot\varphi^2} = \frac{\rho_0}{2V(\varphi)a^3}\,. \tag{22}$$

Therefore the energy density and pressure are given by

$$\rho = \frac{\rho_0}{a^3}\,, \quad p = 0\,. \tag{23}$$

which is exactly the behavior of the pressureless dust or the cold dark matter. It should be noticed that the expression of the energy density is independent of the explicit form of the scalar potential.

It should be noticed that in a single-field inflation, the prediction of the non-linearity parameter is related to the tilt of the power spectrum [3], so if a large local-type non-Gaussianity is confirmed by the future cosmological observations and high level data analysis, it strongly implies that the physics of the early Universe is more complicated than the simple single-field slow-roll inflation. In this paper, we will use $\delta\mathcal{N}$-formalism [13] to calculate the primordial curvature perturbation for the curvaton model with a Lagrange multiplier field. And we find that, in this kind of model, one could get a large non-Gaussinity even if the curvaton dominates the total energy density before it decays. Our paper is organized as follows. In Sec. II, we calculate the non-linearity parameters for the curvaton itself and in Sec. III, we derive in the sudden-decay approximation a non-linear equation that relates the primordial curvature perturbation ζ to the curvaton curvature perturbation ζ_φ. Solving this equation order by order, we obtain the non-linearity parameters f_{NL} and g_{NL} in the sudden-decay approximation and we also compare the results with the usual curvaton model [5]. In Sec. IV, we calculate the pdf and some moments of ζ in the sudden-decay approximation. In the final section, we will give some conclusions and discussions.

II. NON-LINEAR PERTURBATION WITH THE LAGRANGE MULTIPLIER FIELD

The primordial density perturbation can be described in terms of the non-linear curvature perturbation on uniform density hypersurface [14]

$$\zeta(t, \mathbf{x}) = \delta N(t, \mathbf{x}) + \frac{1}{3}\int_{\bar\rho(t)}^{\rho(t,\mathbf{x})} \frac{d\tilde\rho}{\tilde\rho + \tilde p}\,, \tag{24}$$

where $N = \int H dt$ is the amount of local expansion, and ρ^i, p^i are the local energy and pressure respectively. Here, $\bar\rho$ is the homogeneous energy density in the background model, while $\tilde\rho$ and $\tilde p$ is the local density and local pressure.

A. The $L - \lambda\varphi$ model

In this model, we will assume that the constant pressure p is much smaller than the energy density, so the scalar field behaves much like the pressureless dust, thus we have the non-linear curvature perturbation on uniform-curvaton density surfaces is given by [14]

$$\zeta(t, \mathbf{x})_\varphi = \delta N(t, \mathbf{x}) + \int_{\bar\rho_\varphi(t)}^{\rho_\varphi(t,\mathbf{x})} \frac{d\tilde\rho_\varphi}{3\tilde\rho_\varphi}\,. \tag{25}$$

Hence, the density of the scalar field φ on spatially-flat hypersurfaces is given by

$$\rho_\varphi|_{\delta N=0} = e^{3\zeta_\varphi}\bar{\rho}_\varphi \,. \tag{26}$$

Generally, we can expand any field

$$\varphi = \bar{\varphi} + \sum_{n=1}^{\infty}\frac{1}{n!}\delta_n\varphi \,, \tag{27}$$

where $\bar{\varphi}$ is the homogeneous background filed. On the other sider, the quantum fluctuations in a weakly coupled field could be well described by a Gaussian random field [15]. So for such fields, one can only keep the first order perturbation $\delta_1\varphi$ and the higher order perturbations $\delta_n\varphi$ for $n > 1$ that describe non-Gassian perturbations of any field could be neglected. However, here we also want to estimate the effect of the non-linear quantum fluctuations in the curvaton field and Lagrange multiplier field at Hubble exit during inflation, we will keep to the third order of the fluctuations as

$$\varphi_* = \bar{\varphi}_* + \delta_1\varphi_* + \frac{1}{2}\delta_2\varphi_* + \frac{1}{6}\delta_3\varphi_* \tag{28}$$

$$\lambda_* = \bar{\lambda}_* + \delta_1\lambda_* + \frac{1}{2}\delta_2\lambda_* + \frac{1}{6}\delta_3\lambda_* \tag{29}$$

where $*$ denotes that the quantities are evaluated at the Hubble exit during inflation. Therefore, we get the density fluctuation of the curvaton as

$$\rho_{\varphi*} = \bar{\rho}_{\varphi*} + 2V\left(\delta_1\lambda_* + \frac{1}{2}\delta_2\lambda_* + \frac{1}{6}\delta_3\lambda_*\right) \,, \tag{30}$$

where $\bar{\rho}_{\varphi*} = 2V(K_X + \lambda_*) - p \approx 2V(K_X + \lambda_*)$. Therefore, order by order, from Eq. (26) we have

$$\delta_1\rho_{\varphi*} = 2V\delta_1\lambda* \,, \quad \delta_2\rho_{\varphi*} = 2V\delta_2\lambda* \,, \quad \delta_3\rho_{\varphi*} = 2V\delta_3\lambda* \,, \tag{31}$$

and we also have $e^{3\zeta_\varphi} = \rho_{\varphi*}/\bar{\rho}_{\varphi*}$, then

$$\zeta_{\varphi 1} = \frac{2V}{3\bar{\rho}_{\varphi*}}\delta_1\lambda_* \,, \tag{32}$$

$$\zeta_{\varphi 2} = \frac{2V}{3\bar{\rho}_{\varphi*}}\delta_2\lambda_* - 3\zeta_{\varphi 1}^2 = 3\left(a_1 - 1\right)\zeta_{\varphi 1}^2 \,, \tag{33}$$

$$\zeta_{\varphi 3} = \frac{2V}{3\bar{\rho}_{\varphi*}}\delta_3\lambda_* + 9(2 - 3a_1)\zeta_{\varphi 1}^3 = 9(2 - 3a_1 + b_1)\zeta_{\varphi 1}^3 \,, \tag{34}$$

where we have defined

$$a_1 = \frac{\bar{\rho}_*}{2V}\frac{\delta_2\lambda_*}{(\delta_1\lambda_*)^2} \,, \quad b_1 = \frac{\bar{\rho}_*^2}{4V^2}\frac{\delta_3\lambda_*}{(\delta_1\lambda_*)^3} \,, \tag{35}$$

to estimate the effect of the non-linear quantum fluctuations of the Lagrange multiplier field, and if $a_1 \sim 0$ and $b_1 \sim 0$, this field is almost Gaussian. Using Eqs. (32)-(34), one can express the non-linearity parameters for the curvaton perturbation analogous to Eq. (3) as

$$f_{NL}^{\varphi} = \frac{5}{2}(a_1 - 1) \,, \quad g_{NL}^{\varphi} = \frac{25}{6}(2 - 3a_1 + b_1) \,. \tag{36}$$

Here we find $f_{NL}^{\varphi} = -5/2$ and $g_{NL}^{\varphi} = 25/3$ for a Gaussian λ field, while curvaton field itself could be Gaussian or non-Gaussian, and we also have the relation $10f_{NL}^{\varphi} + 3g_{NL}^{\varphi} = 0$. It is worth to note that in this model, the fluctuation of the curvaton field do not contribute to the non-linearity parameters since V is a constant.

B. The $D - \lambda\varphi$ model

In this model, the density fluctuation is given by

$$\rho_{\varphi*} = \bar{\rho}_{\varphi*}\left(1 + \bar{\lambda}_*^{-1}\delta\lambda_* + \bar{V}_*^{-1}\delta V_*\right) \,, \tag{37}$$

where $\bar{V}_* = V(\bar{\varphi}_*)$, $\bar{\rho}_{\varphi *} = 2\bar{V}_*\bar{\lambda}_*$,

$$\delta\lambda_* = \delta_1\lambda_* + \frac{1}{2}\delta_2\lambda_* + \frac{1}{6}\delta_3\lambda_* \,, \tag{38}$$

and

$$\begin{aligned} \delta V_* &= \bar{V}_*'\delta_1\varphi_* + \frac{1}{2}\bar{V}_*'\delta_2\varphi_* + \frac{1}{2}\bar{V}_*''(\delta_1\varphi_*)^2 \\ &+ \frac{1}{6}\bar{V}_*'\delta_3\varphi_* + \frac{1}{2}\bar{V}_*''\delta_1\varphi_*\delta_2\varphi_* + \frac{1}{6}\bar{V}_*'''(\delta_1\varphi_*)^3 \,, \end{aligned} \tag{39}$$

where the prime denotes the derivative with respect to φ. From Eq. (37), one can see that both the fluctuation of λ and φ fields contribute to the fluctuation of the density, so in the following, we will consider two limit case: $\delta V_* = 0$ and $\delta\lambda_* = 0$ to close and open one of them and clearly illustrate the contribution of each field to the non-linearity parameters. In the case of $\delta V_* = 0$, we get the the curvature perturbation as

$$\zeta_{\varphi 1} = \frac{\delta_1\lambda_*}{3\bar{\lambda}_*} \,, \tag{40}$$

$$\zeta_{\varphi 2} = \frac{\delta_2\lambda_*}{3\bar{\lambda}_*} - 3\zeta_{\varphi 1}^2 = 3(a_2 - 1)\zeta_{\varphi 1}^2 \,, \tag{41}$$

$$\zeta_{\varphi 3} = \frac{\delta_3\lambda_*}{3\bar{\lambda}_*} + 9(2 - 3a_2)\zeta_{\varphi 1}^3 = 9(2 - 3a_2 + b_2)\zeta_{\varphi 1}^3 \,, \tag{42}$$

where $a_2 = \bar{\lambda}_*\delta_2\lambda_*/(\delta_1\lambda_*)^2$ and $b_2 = \bar{\lambda}_*^2\delta_3\lambda_*/(\delta_1\lambda_*)^3$. Here, one can see that these equations are the same as Eqs. (32)-(34) except for the definition of a_i and b_i. While in the case of $\delta\lambda_* = 0$, we get

$$\zeta_{\varphi 1} = \frac{\bar{V}_*'}{3\bar{V}_*}\delta_1\varphi_* \,, \tag{43}$$

$$\zeta_{\varphi 2} = \frac{\bar{V}_*'}{3\bar{V}_*}\delta_2\varphi_* + 3\left(\frac{\bar{V}_*''\bar{V}_*}{\bar{V}_*'^2} - 1\right)\zeta_{\varphi 1}^2 = 3\left(a_3 + \frac{\bar{V}_*''\bar{V}_*}{\bar{V}_*'^2} - 1\right)\zeta_{\varphi 1}^2 \,, \tag{44}$$

$$\begin{aligned} \zeta_{\varphi 3} &= \frac{\bar{V}_*'}{3\bar{V}_*}\delta_3\varphi_* + 9\left(2 - 3a_3 - 3(1 - a_3)\frac{\bar{V}_*''\bar{V}_*}{\bar{V}_*'^2} + \frac{\bar{V}_*'''\bar{V}_*^2}{\bar{V}_*'^3}\right)\zeta_{\varphi 1}^3 \\ &= 9\left(2 - 3a_3 + b_3 - 3(1 - a_3)\frac{\bar{V}_*''\bar{V}_*}{\bar{V}_*'^2} + \frac{\bar{V}_*'''\bar{V}_*^2}{\bar{V}_*'^3}\right)\zeta_{\varphi 1}^3 \,, \end{aligned} \tag{45}$$

where

$$a_3 = \frac{\bar{V}_*}{\bar{V}_*'}\frac{\delta_2\varphi_*}{(\delta_1\varphi_*)^2} \,, \quad b_3 = \frac{\bar{V}_*^2}{\bar{V}_*'^2}\frac{\delta_3\varphi_*}{(\delta_1\varphi_*)^3} \,. \tag{46}$$

Then, using Eqs. (43)-(45), one can express the non-linearity parameters for the curvaton perturbation analogous to Eq. (3) as

$$f_{NL}^{\varphi} = \frac{5}{2}\left(a_3 + \frac{\bar{V}_*''\bar{V}_*}{\bar{V}_*'^2} - 1\right) \,, \quad g_{NL}^{\varphi} = \frac{25}{6}\left(2 - 3a_3 + b_3 - 3(1 - a_3)\frac{\bar{V}_*''\bar{V}_*}{\bar{V}_*'^2} + \frac{\bar{V}_*'''\bar{V}_*^2}{\bar{V}_*'^3}\right) \,. \tag{47}$$

Now, let's forget about the a_3 and b_3 for a while, and take the function V as the power of φ, namely, $V \sim \varphi^n$, then the non-linearity parameters becomes

$$f_{NL}^{\varphi} = -\frac{5}{2n} \,, \quad g_{NL}^{\varphi} = \frac{25}{3n^2} \,, \tag{48}$$

which could be larger when n is small. And here, if we take $V \sim e^{m\varphi}$, these parameters would be vanished. With Eq. (48), one can find the following relation

$$10 f_{NL}^{\varphi} + 3n g_{NL}^{\varphi} = 0 \,. \tag{49}$$

It should be noticed that, the result Eq. (48) is evidently distinguishing with that in Ref. [16], in which the author considered a simple power-law potential of the curvaton, i.e. $V \sim \varphi^n$, but the equation of state of the curvaton scaclar depends on the value of n as $w = p/\rho = (n-2)/(n+2)$ in their situation. However, in our model, the pressure is always vanished. In a special case $n = 2$, both our result and that in Ref. [16] are coincident with the result for the quadratic potential of the curvaton [5]. Of course, one can take the other forms of the function V, like $V \sim \cosh(m\varphi)$ to generate large non-Gassuaianity even when the curvaton density dominates the universe, as long as $m\varphi_* \ll 1$:

$$\begin{aligned} \tilde{f}^{\varphi}_{NL} &= \frac{5}{2\sinh^2(m\varphi_*)} \approx \frac{5}{2(m\varphi_*)^2}\,, &(50)\\ \tilde{g}^{\varphi}_{NL} &= -\frac{25}{3\sinh^2(m\varphi_*)} \approx -\frac{25}{3(m\varphi_*)^2}\,, &(51)\end{aligned}$$

and one can also find the relation

$$10\tilde{f}^{\varphi}_{NL} + 3\tilde{g}^{\varphi}_{NL} = 0\,. \tag{52}$$

III. SUDDEN-DECAY APPROXIMATION AND THE PRIMORDIAL CURVATURE PERTURBATION

We assume that the curvaton decays on a uniform-total energy density hypersurface and thus from Eq. (24) the perturbed expansion on this hypersurface is $\delta N = \zeta$, where ζ is the total curvature perturbations at curvaton decay surface. And on this surface, we have

$$\rho_r(t_d, \mathbf{x}) + \rho_\varphi(t_d, \mathbf{x}) = \bar{\rho}(t_d)\,. \tag{53}$$

Here, we assume that all the curvaton decay products are relativistic, then ζ is conserved after the curvaton decay. The local curvaton and radiation density on this decay surface may be inhomogeneous and they have a conserved curvature perturbations when they do not have interactions with each other [14] :

$$\zeta_i = \delta N + \frac{1}{3}\int_{\bar{\rho}_i}^{\rho_i} \frac{d\tilde{\rho}_i}{\tilde{\rho}_i + \tilde{p}_i}\,. \tag{54}$$

Thus, the curvature perturbation related to radiations ($p_r = \rho_r/3$) is

$$\zeta_r = \zeta + \frac{1}{4}\ln\left(\frac{\rho_r}{\bar{\rho}_r}\right)\,, \quad \text{or} \quad \rho_r = \bar{\rho}_r e^{4(\zeta_r - \zeta)}\,, \tag{55}$$

and

$$\zeta_\varphi = \zeta + \frac{1}{3}\ln\left(\frac{\rho_r}{\bar{\rho}_r}\right)\,, \quad \text{or} \quad \rho_r = \bar{\rho}_r e^{3(\zeta_\varphi - \zeta)}\,. \tag{56}$$

Therefore, from Eq. (53) we have the following relation

$$(1 - \Omega_{\varphi,d})e^{4(\zeta_r - \zeta)} + \Omega_{\varphi,d}e^{3(\zeta_\varphi - \zeta)} = 1\,, \tag{57}$$

where $\Omega_{\varphi,d} = \bar{\rho}_\varphi/(\bar{\rho}_r + \bar{\rho}_\varphi)$ is the dimensionless density parameter for the curvaton at the decay time t_d. Here, we take the sudden decay approximation for the curvaton, namely, the curvaton particles instantaneous decay into radiations. And for simplicity, we will ignore the small curvature perturbation in the radiation fluid before the curvaton decays, i.e. $\zeta_r = 0$. Then, order by order from Eq. (57), we have

$$\begin{aligned} \zeta_1 &= f_d \zeta_{\varphi 1}\,, &(58)\\ \zeta_2 &= \left[\frac{3}{f_d}\left(\frac{2}{5}f^{\varphi}_{NL} + 1\right) - 2 - f_d\right]\zeta_1^2\,, &(59)\\ \zeta_3 &= \left[\frac{54}{f_d^2}\left(\frac{g^{\varphi}_{NL}}{25} + \frac{f^{\varphi}_{NL}}{5} + \frac{1}{6}\right) - \frac{18}{f_d}\left(\frac{2}{5}f^{\varphi}_{NL} + 1\right) - \frac{18}{5}f^{\varphi}_{NL} - 4 + 10f_d + 3f_d^2\right]\zeta_1^3\,, &(60)\end{aligned}$$

where

$$f_d = \frac{3\Omega_{\varphi,d}}{4 - \Omega_{\varphi,d}}\,, \tag{61}$$

is called the curvature perturbation transfer efficiency, see Ref. [5]. Therefore, the non-linearity parameters f_{NL} and g_{NL} are given by Eq. (3) as

$$f_{NL} = \frac{1}{f_d}\left(f^{\varphi}_{NL} + \frac{5}{2}\right) - \frac{5(2+f_d)}{6}\,, \tag{62}$$

$$g_{NL} = \frac{1}{f_d^2}\left(g^{\varphi}_{NL} + 5f^{\varphi}_{NL} + \frac{25}{6}\right) - \frac{25}{3f_d}\left(\frac{2}{5}f^{\varphi}_{NL} + 1\right) - \frac{5}{3}f^{\varphi}_{NL} + \frac{25}{54}\left(10f_d + 3f_d^2 - 4\right). \tag{63}$$

In the limit of $f_d \to 1$, namely, the curvaton dominates the total energy density before it decays, we recover $f_{NL} \to f^{\varphi}_{NL}$ and $g_{NL} \to g^{\varphi}_{NL}$. While, in the limit of $f_d \to 0$, one can get large non-Gaussianity as ordinary curvaton models, but this is not the only way to get large non-Gassianity in the $D - \lambda\varphi$ model, because one can get large non-linearity parameters of the curvaton itself f^{φ}_{NL} as we mentioned before.

A. The $L - \lambda\varphi$ model

By using Eqs. (36), (62) and (63), we get

$$f_{NL} = \frac{5a_1}{2f_d} - \frac{5(2+f_d)}{6}\,, \tag{64}$$

$$g_{NL} = \frac{25b_1}{6f_d^2} - \frac{25a_1}{3f_d} - \frac{25a_1}{6} + \frac{25(10f_d + 3f_d^2)}{54} + \frac{125}{54}\,, \tag{65}$$

for the $L-\lambda\varphi$ model. Then, if $f_d \ll a_1$, f_{NL} could be large, but g_{NL} could be large or small depending on the exactly values of a_1, b_1 and f_d. Otherwise, if a_1, b_1 are much smaller than f_d, the terms with the factor a_1 or b_1 could be neglected, then

$$f_{NL} = -\frac{5}{3} - \frac{5}{6}f_d\,, \quad g_{NL} = 25\left(\frac{5f_d}{27} + \frac{f_d^2}{18} + \frac{5}{54}\right). \tag{66}$$

Thus, we have $-5/2 \le f_{NL} < -5/3$ and $125/54 < g_{NL} \le 25/3$ for a Gaussian λ field. And also we have the relation $25f_{NL} + 18g_{NL} = 0$ in the limit of $f_d \to 0$ in this situation.

To illustrate the above analytic study clearly, we plot the non-linearity parameters f_{NL} and g_{NL} as the function of f_d (the transfer efficiency) in Fig. 1 and Fig. 2, and we also plot the results in a usual curvaton model [5] without nonlinear evolution of the curvaton field between the Hubble exit and the moment of its decay with a black dashed curve in these figures.

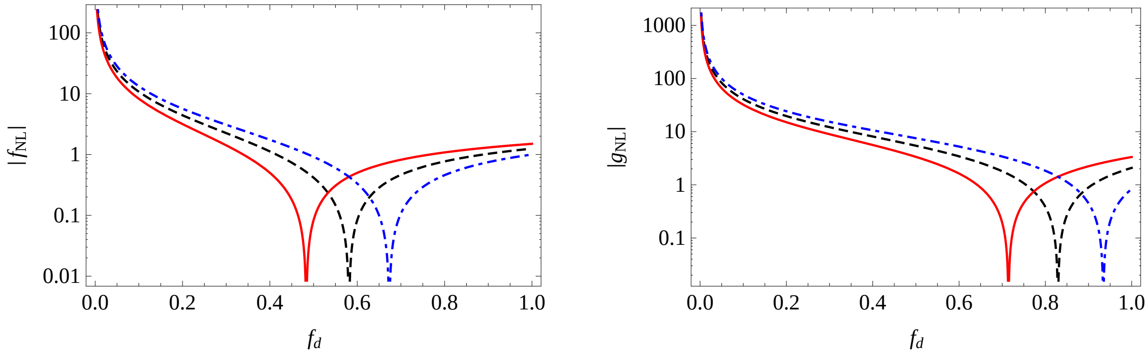

FIG. 1: The non-linearity parameters f_{NL} (left) and g_{NL} (right) as a function of the curvature perturbation transfer efficiency $f_d = \zeta_1/\zeta_{\varphi 1}$ in the $L - \lambda\varphi$ model and the usual curvaton model (black dashed curve). The red solid curve corresponds to $a_1 = 0.4$, while the blue dot-dashed curve corresponds to $a_1 = 0.6$ and here we have set $b_1 = 0$. If $a_1 = 0.5, b_1 = 0$, then the curves predicted in the $L - \lambda\varphi$ model and the usual curvaton model are the same.

From Fig. 1 , one can see that the shape of the curves in the $L-\lambda\varphi$ model are almost the same as that in the usual curvaton model. They would coincide together when $a_1 = 0.5, b_1 = 0$. If b_1 does not vanish, see Fig. 2, the shape of the curves of g_{NL} in the $L - \lambda\varphi$ model are much more different with that in the usual curvaton model when $f_d \to 0$ due to the contribution of the first ($\sim f_d^{-2}$) terms in Eq. (65).

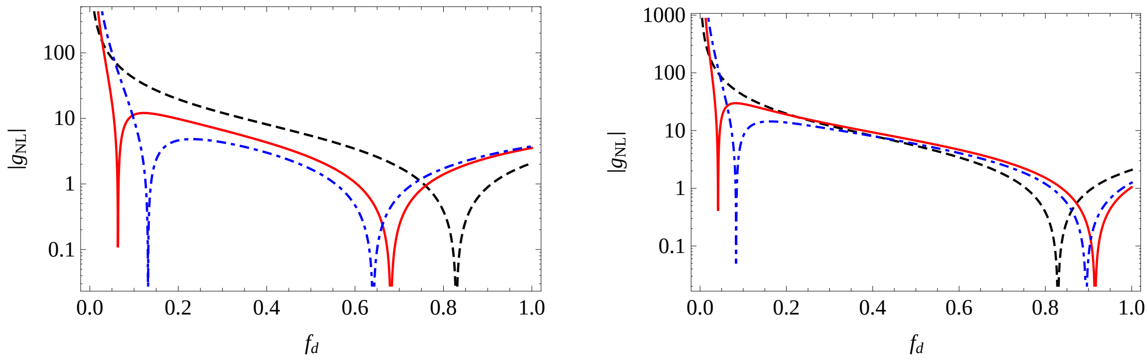

FIG. 2: The non-linearity parameters g_{NL} as a function of the curvature perturbation transfer efficiency $f_d = \zeta_1/\zeta_{\varphi 1}$ with $a = 0.4$(left) and $a = 0.6$(right) in the $L - \lambda\varphi$ model and the usual curvaton model (black dashed curve). The red solid curve corresponds to $b_1 = 0.05$, while the blue dot-dashed curve corresponds to $b_1 = 0.1$ in both figures.

B. The $D - \lambda\varphi$ model

In the case of $\delta V_* = 0$, the result is the same as that in the $L - \lambda\varphi$ model except for the definition of a_i and b_i, so we will focus on the case of $\delta\lambda_* = 0$ in this model. By using Eqs. (47), (62) and (63), we get

$$f_{NL} = \frac{5}{2f_d}\left(a_3 + \frac{\bar{V}''_*\bar{V}_*}{\bar{V}'^2_*}\right) - \frac{5(2+f_d)}{6}\,, \tag{67}$$

$$g_{NL} = \frac{25}{6f_d^2}\left(b_3 + 3a_3\frac{\bar{V}''_*\bar{V}_*}{\bar{V}'^2_*} + \frac{\bar{V}'''_*\bar{V}^2_*}{\bar{V}'^3_*}\right) - \left(\frac{25}{3f_d} + \frac{25}{6}\right)\left(a_3 + \frac{\bar{V}''_*\bar{V}_*}{\bar{V}'^2_*}\right) + \frac{25(10f_d + 3f_d^2)}{54} + \frac{125}{54}\,. \tag{68}$$

Now, lets forget about the a_3 and b_3 for a while, and take the function $V \sim \varphi^n$, then we have

$$f_{NL} = \frac{5}{2f_d}\left(\frac{n-1}{n}\right) - \frac{5}{3} - \frac{5}{6}f_d\,, \tag{69}$$

$$g_{NL} = 25\left[\frac{(n-2)(n-1)}{6f_d^2 n^2} - \left(\frac{1}{3f_d} + \frac{1}{6}\right)\left(\frac{n-1}{n}\right) + \frac{5f_d}{27} + \frac{f_d^2}{18} + \frac{5}{54}\right]\,, \tag{70}$$

which could be larger when n is small. Of course, one can also get large non-Gaussianity with $f_d \ll 1$ when $n \neq 1$. If $n = 1$, then f_{NL} and g_{NL} have the same value as that in the $L - \lambda\varphi$ model, see Eq. (66). If $n = 2$ and in the limit of $f_d \to 0$, we have $f_{NL} \to 5/(4f_d)$, $g_{NL} \to -25/(6f_d)$ and the relation $10f_{NL} + 3g_{NL} = 0$, which means g_{NL} has the same order as f_{NL}. However, if $n \neq 1, 2$, we have

$$f_{NL} \to \frac{5}{2f_d}\left(\frac{n-1}{n}\right)\,, \quad g_{NL} \to \frac{25(n-2)(n-1)}{6f_d^2 n^2}\,, \tag{71}$$

in the limit of $f_d \to 0$. And, this time

$$g_{NL} = \frac{2(n-2)}{3(n-1)}f_{NL}^2\,, \tag{72}$$

which is much larger. The non-linearity parameters f_{NL} and g_{NL} as the function of f_d are plotted in Fig. 3 with $V \sim \varphi^n$, and the results in a usual curvaton model with linear evolution of the curvaton field between the Hubble exit and the moment of its decay are plotted with black dashed curves in these figures. From Fig. 3, one can see that the shape of the curves are very similar except for a small value of n with red solid curves, which means one can get large non-Gaussianity ($|f_{NL}| \gg 1$) even if the curvaton dominates the total energy density before it decays ($f_d \to 1$) by setting a small n, e.g. $n = 0.1$.

If we take the function $V \sim \cosh(m\varphi)$, then we get

$$\tilde{f}_{NL} = \frac{5}{2f_d\tanh^2(m\varphi_*)} - \frac{5(2+f_d)}{6}\,, \tag{73}$$

$$\tilde{g}_{NL} = 25\left[\frac{1}{6f_d^2\tan^2(m\varphi_*)} - \left(\frac{1}{3f_d} + \frac{1}{6}\right)\frac{1}{\tanh^2(m\varphi_*)} + \frac{1}{54}\left(10f_d + 3f_d^2 + 5\right)\right]\,. \tag{74}$$

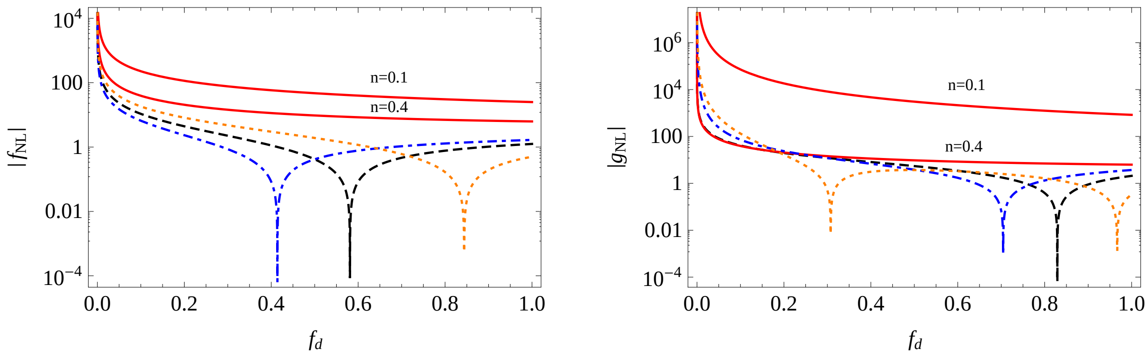

FIG. 3: The non-linearity parameters f_{NL} (left) and g_{NL} (right) as a function of the curvature perturbation transfer efficiency $f_d = \zeta_1/\zeta_{\varphi 1}$ in the case of $\delta\lambda_* = 0$ in the $D - \lambda\varphi$ model with $V \sim \varphi^n$ and the usual curvaton model (black dashed curve). The red solid curve corresponds to $n = 0.1, 0.4$ from top to bottom, while the blue dot-dashed curve corresponds to $n = 1.5$ and the orange dotted curve corresponds to $n = 5$. If $n = 2$, then the curves in the $D - \lambda\varphi$ model will coincide with that in the usual curvaton model. Here we have set $a_3 = b_3 = 0$ for simplicity.

As we mentioned before, when $m\varphi_* \ll 1$, $\tilde{f}_{NL}$ and $\tilde{g}_{NL}$ could be larger even when $f_d = 1$. Taking the limit of $f_d \to 0$, we get

$$\tilde{f}_{NL} \to \frac{5}{2 f_d \tanh^2(m\varphi_*)} \,, \quad \tilde{g}_{NL} \to \frac{25}{6 f_d^2 \tanh^2(m\varphi_*)} \,, \tag{75}$$

and the relation

$$\tilde{g}_{NL} = \frac{2}{3} \tanh^2(m\varphi_*) \tilde{f}_{NL}^2 \,. \tag{76}$$

The non-linearity parameters $\tilde{f}_{NL}$ and $\tilde{g}_{NL}$ as the function of f_d are plotted in Fig. 4 with $V \sim \cosh(m\varphi)$. Again, the black dashed curves in these figures represent the results in a usual curvaton model with linear evolution of the curvaton field between the Hubble exit and the moment of its decay, and the shape of the curves are not similar. For a small value of $m\varphi_* = 0.1$ with red solid curves in the left figure, one can get large non-Gaussianity ($|f_{NL}| \gg 1$) even if the curvaton dominates the total energy density before it decays ($f_d \to 1$).

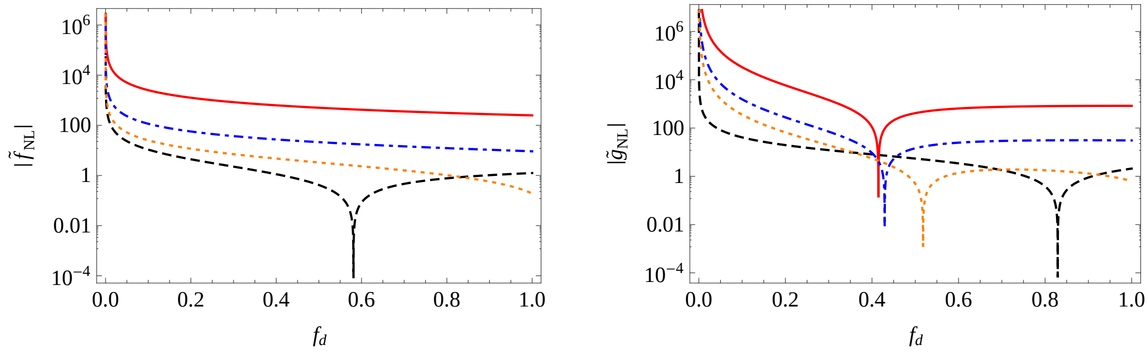

FIG. 4: The non-linearity parameters f_{NL} (left) and g_{NL} (right) as a function of the curvature perturbation transfer efficiency $f_d = \zeta_1/\zeta_{\varphi 1}$ in the case of $\delta\lambda_* = 0$ in the $D - \lambda\varphi$ model with $V \sim \cos(m\varphi)$ and the usual curvaton model (black dashed curve). The red solid curve corresponds to $m\varphi_* = 0.1$, while the blue dot-dashed curve corresponds to $m\varphi_* = 0.5$ and the orange dotted curve corresponds to $m\varphi_* = 2.0$. Here we have set $a_3 = b_3 = 0$ for simplicity.

IV. PROBABILITY DENSITY FUNCTION

In this section, we will follow the method in [15] to calculate the probability density function (pdf) of curvature perturbation. At first, we shall briefly review this method. Let's assume there are two random variables y and z, and the functional dependence of z on y is $z = z(y)$, which is a bijection. If the pdf of y is $\tilde{f}(y)$, then the probability of z being in the interval (z_1, z_2) is given by

$$P(z_1 < z < z_2) = \int_{z_1}^{z_2} \left|\frac{dy}{dz}\right| \tilde{f}(y) dz \,, \tag{77}$$

where the absolute value is need when $y(z)$ is a decreasing function. Hence, the pdf of z is

$$f(z) = \left|\frac{dy(z)}{dz}\right| \tilde{f}[y(z)] \,, \tag{78}$$

where the derivative could be replaced by the Jacobian determinant in the multi-variable case.

Since the first order perturbation ζ_1 only depends linearly on the initial Gaussian field perturbation, one can take ζ_1 as a Gaussian "reference" variable with mean $\mu_{\zeta_1} = 0$. In the sudden decay approximation, we have found an analytic functional dependence $\zeta = \zeta(\zeta_1)$, but the mapping is not always a bijection. Calling these values ζ_{1i}, one can calculate the pdf of the non-linear primordial curvature perturbation

$$f(\zeta) = \sum_i \left|\frac{d\zeta_1}{d\zeta}\right|_{\zeta_1 = \zeta_{1i}} f_g(\zeta_{1i}) \,, \tag{79}$$

where $f(\zeta_1)$ is the Gaussian pdf with mean $\mu = 0$ and variance $\sigma^2 = \sigma^2_{\zeta_1}$:

$$f_g(\zeta_1) = \frac{1}{\sqrt{2\pi\sigma^2_{\zeta_1}}} e^{-\zeta_1^2/(2\sigma^2_{\zeta_1})} \,. \tag{80}$$

For simplicity, in the rest of this section, we will neglect all the non-linear fluctuation of the initial field, namely, we will set $a_i = b_i = 0$ in all models.

Actually, the non-Gaussianity could be described quantitatively by calculating the moments of the pdf and

$$m_z(i) = \int (z - \mu)^i f(z) dz \,, \tag{81}$$

is called the i^{th} moment. Here, the mean μ can be calculated as

$$\mu = \int z f(z) dz \,, \tag{82}$$

where the pdf $f(z)$ satisfies $\int f(z)dz = 1$. Conventionally, the second moment is the variance (σ_z^2), the third moment is called skewness, and the fourth moment kurtosis. For a Gaussian pdf, any odd moment (with $i \geq 3$) is zero, since the probability density is symmetric around the mean, while the even moments could be easily calculated by partial integrating, e.g. $m(4) = 3\sigma^4$, $m(6) = 15\sigma^6$, $m(8) = 105\sigma^8$, $m(10) = 945\sigma^{10}$, $m(12) = 10395\sigma^{12}$, etc., see Ref. [15]. Any departure from these values indicates the pdf is non-Gaussian, namely, there is an asymmetric deviation from Gaussianity, if odd moments are not zero, and if the pdf is more (or less) sharply peaked than the Gaussian if even moments are smaller (or larger) than that in the Gaussian case. Therefore, the set of moments encodes the same information of non-Gaussianity as the fully non-linear ζ or its expansion. Next, we will calculate the pdf and illustrate some moments of the pdf in our models.

A. The $L - \lambda\varphi$ model

From Eqs. (26), (30), (32) and (58), we have

$$e^{3\zeta_\varphi} = 1 + \frac{3\zeta_1}{f_d} \,. \tag{83}$$

While, from Eq. (57) with $\zeta_r = 0$, we have

$$e^{3\zeta_\varphi} = \frac{3 + f_d}{4f_d} e^{3\zeta} + \frac{3f_d - 3}{4f_d} e^{-\zeta} \,. \tag{84}$$

Thus, combing Eqs. (83) and (84), we get

$$\zeta_1 = \frac{f_d}{3}\left(-1 + \frac{3+f_d}{4f_d}e^{3\zeta} + \frac{3f_d-3}{4f_d}e^{-\zeta}\right) , \tag{85}$$

and

$$\left|\frac{d\zeta_1}{d\zeta}\right| = \frac{3+f_d}{4}e^{3\zeta} + \frac{1-f_d}{4}e^{-\zeta} . \tag{86}$$

Hence, the non-Gaussian probability density function for ζ is

$$f(\zeta) = \frac{1}{\sqrt{2\pi\sigma_{\zeta_1}^2}}\left(\frac{3+f_d}{4}e^{3\zeta} + \frac{1-f_d}{4}e^{-\zeta}\right)\exp\left[-\frac{f_d^2}{9}\left(-1 + \frac{3+f_d}{4f_d}e^{3\zeta} + \frac{3f_d-3}{4f_d}e^{-\zeta}\right)^2 /(2\sigma_{\zeta_1}^2)\right] . \tag{87}$$

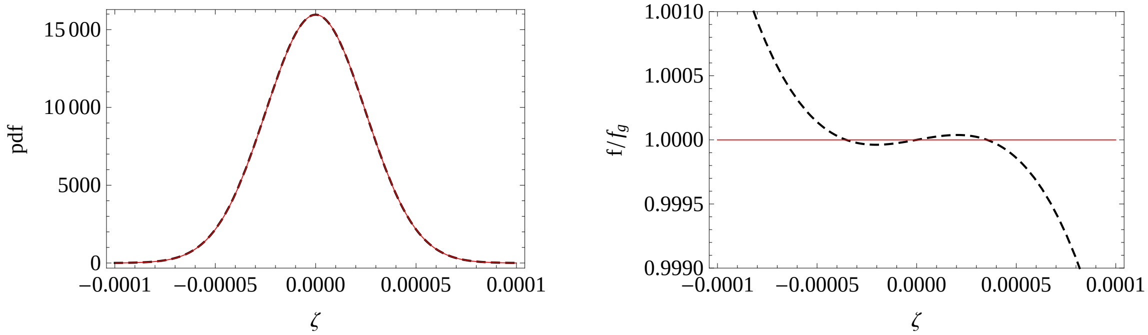

FIG. 5: *The $L - \lambda\varphi$ model.* Left: Pdfs at $f_d = 0.8$, ($f_{NL} = -7/3$). The black dashed curve is the pdf f, while the red solid curve is the Gaussian reference, f_g. Right: The ratio of non-Gaussian pdf to the Gaussian one.

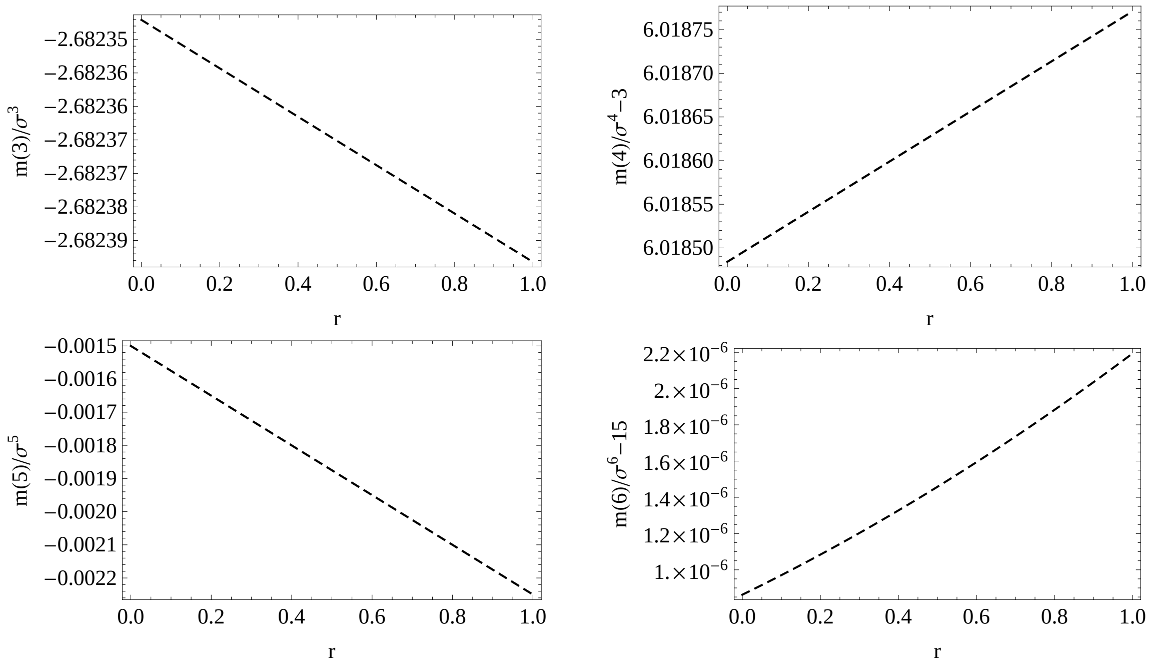

FIG. 6: Third, fourth, fifth and sixth (from left top to right bottom) moments of the pdf of the primordial curvature perturbation ζ as a function of the linear transfer parameter, f_d in the $L - \lambda\varphi$ model.

In Fig. 5, we compare the fully non-linear pdf $f(\zeta)$ to the Gaussian $f_g(\zeta_1)$, and it shows that f is virtually indistinguishable from the Gaussian f_g. But, we also plot f/f_g which reveals the non-Gaussianity in this model. In Fig. 6, we plot the moments from the third up to the sixth one as a function of f_d.

B. The $D - \lambda\varphi$ model

In this model, we will focus on the case of $\delta\lambda_* = 0$. From Eq. (26), (37) and (43), we have

$$e^{3\zeta_\varphi} = 1 + 3\zeta_{\varphi 1} + \frac{9}{2}\frac{\bar{V}''_* V_*}{V'^2_*}(\zeta_{\varphi 1})^2 + \frac{9}{2}\frac{\bar{V}'''_* V^2_*}{V'^3_*}(\zeta_{\varphi 1})^3 . \tag{88}$$

and by combing Eq. (84), we can get the equation for ζ_1 for a given function V. Next, we will consider two types of V and get the non-Gaussian probability density function for ζ by solving the equation as in the $L - \lambda\varphi$ model.

1. $V \sim \varphi^n$

In this case we get the following equation for $\zeta_{\varphi 1}$:

$$\frac{9(n-1)(n-2)}{2n^2}\left(\frac{\zeta_1}{f_d}\right)^3 + \frac{9(n-1)}{2n}\left(\frac{\zeta_1}{f_d}\right)^2 + 3\left(\frac{\zeta_1}{f_d}\right) + d = 0 , \tag{89}$$

where

$$d = 1 - \frac{3+f_d}{4f_d}e^{3\zeta} - \frac{3f_d - 3}{4f_d}e^{-\zeta} . \tag{90}$$

Here we have used Eqs. (84), (88) and (58). If $n = 1$, the results would be the same as that in the $L - \lambda\varphi$ model, while if $n = 2$, we recover the results of the usual curvaton model. For a generic n ($n \neq 1, 2$), the above equation could be rewritten as

$$Y^3 + pY + q = 0 , \tag{91}$$

where we have defined

$$Y = \frac{\zeta_1}{f_d} + \frac{n}{3(n-2)} , \tag{92}$$

$$p = \frac{n^2(n-3)}{3(n-2)^2(n-1)} , \tag{93}$$

$$q = \frac{2n^2}{9(n-2)}\left(\frac{d}{n-1} - \frac{n}{(n-1)(n-2)} + \frac{n}{3(n-2)^2}\right) . \tag{94}$$

Define

$$D = \left(\frac{p}{3}\right)^3 + \left(\frac{q}{2}\right)^2 , \tag{95}$$

then, the number of real roots of the Eq. (91) depends on the sign of D. It should be noticed that if $n > 3$ or $n < 1$, p is positive and then D is also positive. So, in this case, we have only one real root of the Eq. (91):

$$Y_1 = u_+^{1/3} + u_-^{1/3} , \quad u_\pm = \frac{-q}{2} \pm D^{1/2} , \tag{96}$$

and

$$\left|\frac{d\zeta_1}{d\zeta}\right| = \frac{Q}{2\sqrt{D}}\left|u_-^{1/3} - u_+^{1/3}\right| . \tag{97}$$

where

$$Q = \frac{n^2\left[(3+f_d)e^{3\zeta} + (1-f)e^{-\zeta}\right]}{18|n-1||n-2|} . \tag{98}$$

Hence, the non-Gaussian probability density function for ζ is

$$f(\zeta)\Big|_{D>0} = \frac{1}{\sqrt{2\pi\sigma^2_{\zeta_1}}}\left(\frac{Q|u_-^{1/3} - u_+^{1/3}|}{2\sqrt{D}}\right)\exp\left[-\frac{f_d^2}{2\sigma^2_{\zeta_1}}\left(u_+^{1/3} + u_-^{1/3} - \frac{n}{3(n-2)}\right)^2\right] . \tag{99}$$

If $1 < n < 3$ and $n \neq 2$, there could be some regions $\zeta \in (\zeta_a, \zeta_b)$, in which $D < 0$ and $D|_{\zeta=\zeta_a} = D|_{\zeta=\zeta_b} = 0$. So, for completeness, we will give the pdf for ζ in these regions in the following. If $D = 0$, we have three real roots of the Eq. (91) and two of them are equal:

$$Y_1 = 2\left(\frac{-q}{2}\right)^{1/3}, \quad Y_2 = Y_3 = \left(\frac{q}{2}\right)^{1/3}, \tag{100}$$

and then, we have

$$\left|\frac{d\zeta_1^{(1)}}{d\zeta}\right| = Q\left|\left(\frac{-q}{2}\right)^{-2/3}\right|, \quad \left|\frac{d\zeta_1^{(2)}}{d\zeta}\right| = \frac{Q}{2}\left|\left(\frac{q}{2}\right)^{-2/3}\right|. \tag{101}$$

Hence, the non-Gaussian probability density function for ζ is

$$\begin{aligned} f(\zeta)\Big|_{D=0} &= \frac{Q}{\sqrt{2\pi\sigma_{\zeta_1}^2}}\Bigg\{\left|\left(\frac{-q}{2}\right)^{-2/3}\right|\exp\left[-\frac{f_d^2}{2\sigma_{\zeta_1}^2}\left(2\left(\frac{-q}{2}\right)^{1/3} - \frac{n}{3(n-2)}\right)^2\right] \\ &+ \frac{1}{2}\left|\left(\frac{q}{2}\right)^{-2/3}\right|\exp\left[-\frac{f_d^2}{2\sigma_{\zeta_1}^2}\left(\left(\frac{q}{2}\right)^{1/3} - \frac{n}{3(n-2)}\right)^2\right]\Bigg\}. \end{aligned} \tag{102}$$

And, if $D < 0$, we have three different real roots of the Eq. (91):

$$Y_1 = 2\sqrt{\frac{|p|}{3}}\cos\frac{\theta}{3}, \quad Y_{2,3} = -2\sqrt{\frac{|p|}{3}}\cos\frac{\theta \pm \pi}{3}, \tag{103}$$

where

$$\theta = \arccos\left[\frac{-q}{2}\left(\frac{|p|}{3}\right)^{-3/2}\right]. \tag{104}$$

Thus

$$\left|\frac{d\zeta_1^{(1)}}{d\zeta}\right| = Q\sin\frac{\theta}{3}\sin^{-1}\theta\left(\frac{|p|}{3}\right)^{-1}, \tag{105}$$

$$\left|\frac{d\zeta_1^{(2,3)}}{d\zeta}\right| = Q\sin\frac{\theta \pm \pi}{3}\sin^{-1}\theta\left(\frac{|p|}{3}\right)^{-1}. \tag{106}$$

Hence, the non-Gaussian probability density function for ζ is

$$\begin{aligned} f(\zeta)\Big|_{D<0} &= \frac{3Q}{\sqrt{2\pi\sigma_{\zeta_1}^2}|p\sin\theta|}\Bigg\{\left|\sin\frac{\theta}{3}\right|\exp\left[-\frac{f_d^2}{2\sigma_{\zeta_1}^2}\left(2\sqrt{\frac{|p|}{3}}\cos\frac{\theta}{3} - \frac{n}{3(n-2)}\right)^2\right] \\ &+ \sum_{\pm}\left|\sin\frac{\theta \pm \pi}{3}\right|\exp\left[-\frac{f_d^2}{2\sigma_{\zeta_1}^2}\left(2\sqrt{\frac{|p|}{3}}\cos\frac{\theta \pm \pi}{3} + \frac{n}{3(n-2)}\right)^2\right]\Bigg\}. \end{aligned} \tag{107}$$

In Fig. 7, we compare the fully non-linear pdf $f(\zeta)$ to the Gaussian $f_g(\zeta_1)$ in the case when there is large non-Gaussianity. In one of them, the non-linearity parameter is very large ($f_d = 0.8$, $n = -0.001$, $f_{NL} = 3126$), and this kind of visual comparison reveals the non-Gaussianity, but in another one with ($f_d = 0.8$, $n = -0.0276$, $f_{NL} = 114$), it shows that f is virtually indistinguishable from the Gaussian f_g. But, we also plot f/f_g which reveals the non-Gaussianity in this model. In Tab. I, we give some values of the moments from the third up to the sixth one at $f_d = 0.2, 0.5, 0.8$ for $n = -0.001$ and $n = -0.0267$.

2. $V \sim \cosh(m\varphi)$

In this case, we get the following equation for $\zeta_{\varphi 1}$ from Eq. (84) and (88):

$$\left(\frac{\zeta_1}{f_d}\right)^3 + \left(\frac{\zeta_1}{f_d}\right)^2 + \frac{2\tanh^2(m\varphi_*)}{3}\left(\frac{\zeta_1}{f_d}\right) + \frac{2d\tanh^2(m\varphi_*)}{9} = 0, \tag{108}$$

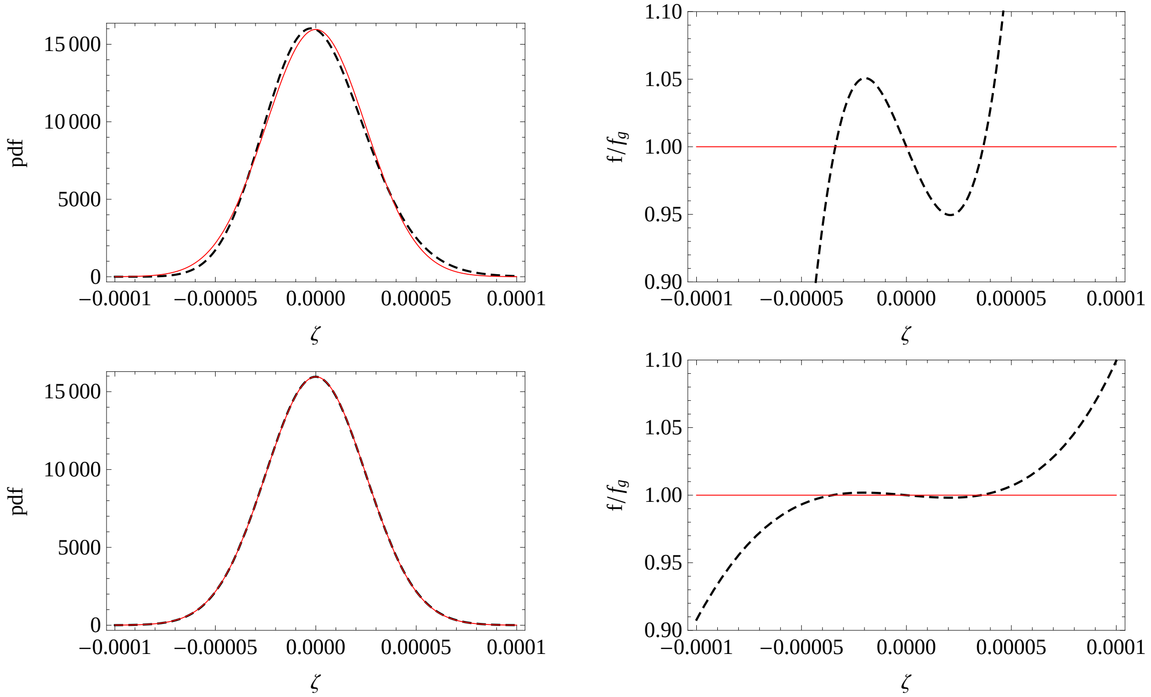

FIG. 7: *The $D-\lambda\varphi$ model with $V \sim \varphi^n$.* Left: Pdfs at $f_d = 0.8$ and $n = -0.001$ (top, $f_{NL} = 3126$), -0.0276 (bottom, $f_{NL} = 114$). The black dashed curve ares the pdfs f, while the red solid curves are the Gaussian reference, f_g. Right: The ratio of non-Gaussian pdf to the Gaussian one with $n = -0.001$ (top), -0.0276 (bottom).

Moment	$n = -0.0010$			$n = -0.0276$		
	$f_d = 0.2$	$f_d = 0.5$	$f_d = 0.8$	$f_d = 0.2$	$f_d = 0.5$	$f_d = 0.8$
$m(3)/\sigma^3$	-6.9688×10^{-3}	-3.5883×10^{-3}	-2.3228×10^{-3}	-3.5297×10^{-4}	-1.4023×10^{-4}	-8.6818×10^{-5}
$m(4)/\sigma^4 - 3$	-2.9970	-2.9980	-2.9982	-2.9985	-2.9985	-2.9985
$m(5)/\sigma^5$	-1.2190×10^{-3}	-5.8153×10^{-4}	-3.6840×10^{-4}	-5.5229×10^{-5}	-2.1891×10^{-5}	-1.3559×10^{-5}
$m(6)/\sigma^6 - 15$	-14.999	-14.999	-14.999	-14.999	-14.999	-14.999

TABLE I: The value of the third, fourth, fifth and sixth moments of the pdf of the primordial curvature perturbation ζ with $n = -0.001, -0.0276$ and $f_d = 0.2, 0.5, 0.8$ in the $D-\lambda\varphi$ model with $\delta\lambda_* = 0$ and $V \sim \varphi^n$.

which could be rewritten as

$$Z^3 + \tilde{p}Z + \tilde{q} = 0\,, \tag{109}$$

where we have defined

$$Z = \frac{\zeta_1}{f_d} + \frac{1}{3}\,, \quad \tilde{p} = \frac{2\tanh^2(m\varphi_*) - 1}{3}\,, \quad \tilde{q} = \frac{2}{27} + \frac{2(d-1)}{9}\tanh^2(m\varphi_*)\,. \tag{110}$$

Thus, the solutions to Eq. (109) are the same as that to Eq. (91) except for the definitions of the coefficients p and q. Define

$$\tilde{D} = \left(\frac{\tilde{p}}{3}\right)^3 + \left(\frac{\tilde{q}}{2}\right)^2\,, \tag{111}$$

whose sign determines the number of roots of the Eq. (109). It should be noticed that if $\tan^2(m\varphi_*) > 1/2$, $\tilde{p}$ is positive and then $\tilde{D}$ is also positive. So, in this case, we have only one real root of the Eq. (109):

$$Z_1 = \tilde{u}_+^{1/3} + \tilde{u}_-^{1/3}\,, \quad \tilde{u}_\pm = \frac{-\tilde{q}}{2} \pm \tilde{D}^{1/2}\,, \tag{112}$$

and

$$\left|\frac{d\zeta_1}{d\zeta}\right| = \frac{\tilde{Q}}{2\sqrt{\tilde{D}}}\left|\tilde{u}_-^{1/3} - \tilde{u}_+^{1/3}\right| . \tag{113}$$

where

$$\tilde{Q} = \frac{\tanh^2(m\varphi_*)}{18}\left[(3+f_d)e^{3\zeta} + (1-f)e^{-\zeta}\right] . \tag{114}$$

Hence, the non-Gaussian probability density function for ζ is

$$f(\zeta)\Big|_{\tilde{D}>0} = \frac{1}{\sqrt{2\pi\sigma_{\zeta_1}^2}}\left(\frac{\tilde{Q}|\tilde{u}_-^{1/3} - \tilde{u}_+^{1/3}|}{2\sqrt{\tilde{D}}}\right)\exp\left[-\frac{f_d^2}{2\sigma_{\zeta_1}^2}\left(\tilde{u}_+^{1/3} + \tilde{u}_-^{1/3} - \frac{1}{3}\right)^2\right] . \tag{115}$$

If $\tan^2(m\varphi_*) < 1/2$, there could be some regions of $\zeta \in (\zeta_a, \zeta_b)$, in which $\tilde{D} < 0$ and $\tilde{D}|_{\zeta=\zeta_a} = \tilde{D}|_{\zeta=\zeta_b} = 0$. So, for completeness, we will give the pdf for ζ in these regions in the following. If $\tilde{D} = 0$, we have three real roots of the Eq. (109) and two of them are equal:

$$Z_1 = 2\left(\frac{-\tilde{q}}{2}\right)^{1/3} , \quad Z_2 = Y_3 = \left(\frac{\tilde{q}}{2}\right)^{1/3} , \tag{116}$$

and then, we have

$$\left|\frac{d\zeta_1^{(1)}}{d\zeta}\right| = \tilde{Q}\left|\left(\frac{-\tilde{q}}{2}\right)^{-2/3}\right| , \quad \left|\frac{d\zeta_1^{(2)}}{d\zeta}\right| = \frac{\tilde{Q}}{2}\left|\left(\frac{\tilde{q}}{2}\right)^{-2/3}\right| . \tag{117}$$

Hence, the non-Gaussian probability density function for ζ is

$$\begin{aligned} f(\zeta)\Big|_{\tilde{D}=0} &= \frac{\tilde{Q}}{\sqrt{2\pi\sigma_{\zeta_1}^2}}\left\{\left|\left(\frac{-\tilde{q}}{2}\right)^{-2/3}\right|\exp\left[-\frac{f_d^2}{2\sigma_{\zeta_1}^2}\left(2\left(\frac{-\tilde{q}}{2}\right)^{1/3} - \frac{1}{3}\right)^2\right]\right. \\ &+ \left.\frac{1}{2}\left|\left(\frac{\tilde{q}}{2}\right)^{-2/3}\right|\exp\left[-\frac{f_d^2}{2\sigma_{\zeta_1}^2}\left(\left(\frac{\tilde{q}}{2}\right)^{1/3} - \frac{1}{3}\right)^2\right]\right\} . \end{aligned} \tag{118}$$

And, for $\tilde{D} < 0$, we have three different real roots of the Eq. (109):

$$Z_1 = 2\sqrt{\frac{|\tilde{p}|}{3}}\cos\frac{\tilde{\theta}}{3} , \quad Z_{2,3} = -2\sqrt{\frac{|\tilde{p}|}{3}}\cos\frac{\tilde{\theta}\pm\pi}{3} , \tag{119}$$

where

$$\tilde{\theta} = \arccos\left[\frac{-\tilde{q}}{2}\left(\frac{|\tilde{p}|}{3}\right)^{-3/2}\right] . \tag{120}$$

Thus

$$\left|\frac{d\zeta_1^{(1)}}{d\zeta}\right| = \tilde{Q}\sin\frac{\tilde{\theta}}{3}\sin^{-1}\tilde{\theta}\left(\frac{|\tilde{p}|}{3}\right)^{-1} , \tag{121}$$

$$\left|\frac{d\zeta_1^{(2,3)}}{d\zeta}\right| = \tilde{Q}\sin\frac{\tilde{\theta}\pm\pi}{3}\sin^{-1}\tilde{\theta}\left(\frac{|\tilde{p}|}{3}\right)^{-1} . \tag{122}$$

Hence, the non-Gaussian probability density function for ζ is

$$\begin{aligned} f(\zeta)\Big|_{\tilde{D}<0} &= \frac{3\tilde{Q}}{\sqrt{2\pi\sigma_{\zeta_1}^2}\,|\tilde{p}\sin\tilde{\theta}|}\left\{\left|\sin\frac{\tilde{\theta}}{3}\right|\exp\left[-\frac{f_d^2}{2\sigma_{\zeta_1}^2}\left(2\sqrt{\frac{|\tilde{p}|}{3}}\cos\frac{\tilde{\theta}}{3} - \frac{1}{3}\right)^2\right]\right. \\ &+ \left.\sum_{\pm}\left|\sin\frac{\tilde{\theta}\pm\pi}{3}\right|\exp\left[-\frac{f_d^2}{2\sigma_{\zeta_1}^2}\left(2\sqrt{\frac{|\tilde{p}|}{3}}\cos\frac{\tilde{\theta}\pm\pi}{3} + \frac{1}{3}\right)^2\right]\right\} . \end{aligned} \tag{123}$$

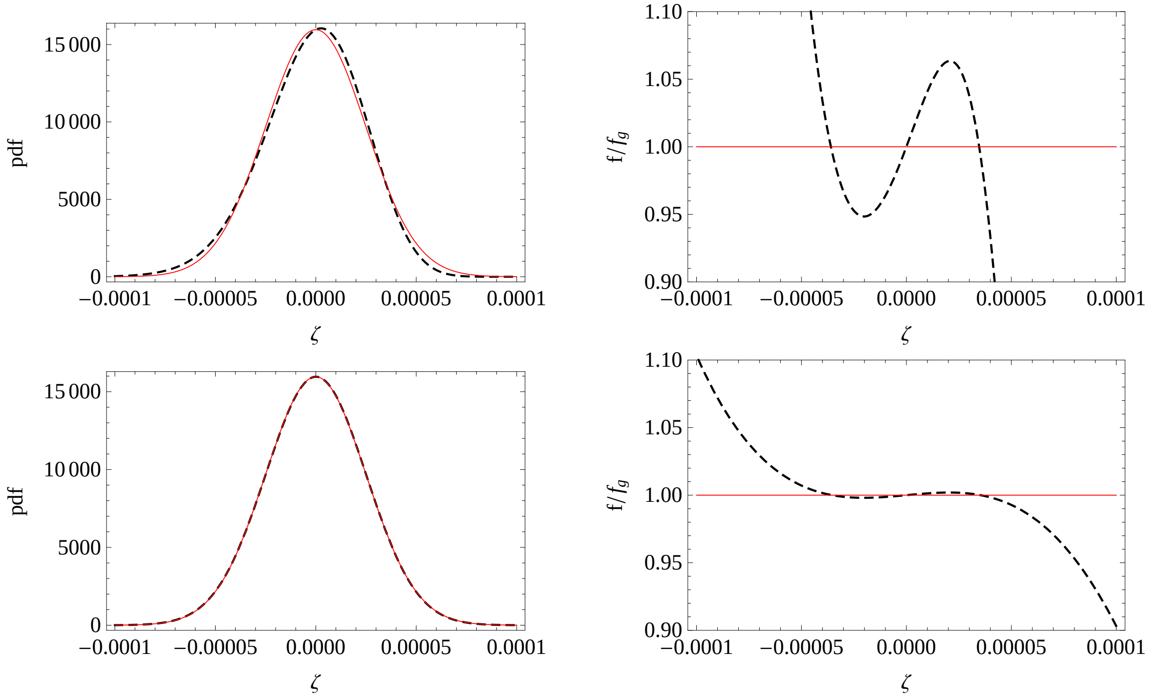

FIG. 8: *The* $D - \lambda\varphi$ *model with* $V \sim \cosh(m\varphi)$. Left: Pdfs at $f_d = 0.8$ and $m\varphi_* = 0.003$ (top, $f_{NL} = 3472$), 0.165 (bottom, $f_{NL} = 114$). The black dashed curve ares the pdfs f, while the red solid curves are the Gaussian reference, f_g. Right: The ratio of non-Gaussian pdf to the Gaussian one with $m\varphi_* = 0.003$ (top), 0.165 (bottom).

Moment	$m\varphi_* = 0.03$			$m\varphi_* = 0.165$		
	$f_d = 0.2$	$f_d = 0.5$	$f_d = 0.8$	$f_d = 0.2$	$f_d = 0.5$	$f_d = 0.8$
$m(3)/\sigma^3$	1.4076×10^{-2}	4.3669×10^{-3}	2.6789×10^{-3}	3.5764×10^{-4}	1.4406×10^{-4}	9.0822×10^{-5}
$m(4)/\sigma^4 - 3$	-2.9931	-2.9977	-2.9982	-2.9985	-2.9985	-2.9985
$m(5)/\sigma^5$	3.4784×10^{-3}	7.4967×10^{-4}	4.3509×10^{-4}	5.5869×10^{-5}	2.2490×10^{-5}	1.4178×10^{-5}
$m(6)/\sigma^6 - 15$	-14.999	-14.999	-14.999	-14.999	-14.999	-14.999

TABLE II: The value of the third, fourth, fifth and sixth moments of the pdf of the primordial curvature perturbation ζ with $m\varphi_* = 0.003, 0.165$ and $f_d = 0.2, 0.5, 0.8$ in the $D - \lambda\varphi$ model with $\delta\lambda_* = 0$ and $V \sim \cosh(m\varphi)$.

In Fig. 8, we compare the fully non-linear pdf $f(\zeta)$ to the Gaussian $f_g(\zeta_1)$ in the case when there is large non-Gaussianity. In one of them, the non-linearity parameter is very large ($f_d = 0.8$, $m\varphi_* = 0.03$, $f_{NL} = 3472$), and this kind of visual comparison reveals the non-Gaussianity, but in another one with ($f_d = 0.8$, $m\varphi_* = 0.165$, $f_{NL} = 114$), it shows that f is virtually indistinguishable from the Gaussian f_g. But, we also plot f/f_g which reveals the non-Gaussianity in this model. In Tab. II, we give some values of the moments from the third up to the sixth one at $f_d = 0.2, 0.5, 0.8$ for $m\varphi_* = 0.03$ and $m\varphi_* = 0.165$.

V. CONCLUSION

We have used $\delta\mathcal{N}$-formalism to calculate the primordial curvature perturbation for the curvaton model with a Lagrange multiplier field in two interesting cases. We have calculate the non-linearity parameters f_{NL} and g_{NL} in the probability density function of the primordial curvature perturbation in the sudden-decay approximation, as well as some moments of it. We find that one can get a large non-Gaussianity in this kind of model even if the curvaton dominates the total energy density before it decays, namely $f_d \to 1$, while in the usual curvaton model with quadratic potential, one can only get a large non-Gaussianity when the curvaton is subdominant, namely in the limit of $f_d \to 0$, see [5]. It should be noticed that the isocurvature perturbations are created when the curvaton fail to dominate the energy density while decaying. So, it will not produce large f_{NL} comparing to that of WMAP by taking account of the constraint of isocurvature perturbations [17]. So, it seems that we have escaped the constraint from isocurvature perturbations and give a large f_{NL} comparable to the result of WMAP. So, the introduction of Lagrange multiplier field will make the the curvaton model much richer, e.g. it also release the form of the potential.

Furthermore, it hase been shown that with the help of a Lagrange multiplier field, one can proposed a way to unify dark matter and dark energy in a single degree of freedom, see [12]. And the Lagrange multiplier modified gravity may lead to cyclic behavior very easily in the cyclic cosmology, and the scenario is much more realistic in the case of scalar cosmology [18]. So, we conclude that the Lagrange multiplier field could play a very interesting and important role in the construction of cosmological models, and it also interesting to study the primordial nonlinear structures and black holes [19] in such kind of curvaton scenario.

Acknowledgments

We would like to thank Anupam Mazumdar and Maxim.Yu.Khlopov for helpful comments and discussions. This work is supported by National Education Foundation of China grant No. 2009312711004 and Shanghai Natural Science Foundation, China grant No. 10ZR1422000.

Appendix A

[1] A. H. Guth, "The Inflationary Universe: A Possible Solution To The Horizon And Flatness Phys. Rev. D **23**, 347 (1981).
A. D. Linde, "A New Inflationary Universe Scenario: A Possible Solution Of The Horizon, Phys. Lett. B **108**, 389 (1982).
A. J. Albrecht and P. J. Steinhardt, "Cosmology For Grand Unified Theories With Radiatively Induced Symmetry Phys. Rev. Lett. **48**, 1220 (1982).

[2] C. J. Feng, X. Z. Li and E. N. Saridakis, Phys. Rev. D **82**, 023526 (2010) [arXiv:1004.1874 [astro-ph.CO]].
C. J. Feng and X. Z. Li, arXiv:0911.3994 [astro-ph.CO].

[3] J. M. Maldacena, JHEP **0305**, 013 (2003) [arXiv:astro-ph/0210603].

[4] D. Wands, Lect. Notes Phys. **738**, 275 (2008) [arXiv:astro-ph/0702187].

[5] A. D. Linde and V. F. Mukhanov, Phys. Rev. D **56**, 535 (1997) [arXiv:astro-ph/9610219].
K. Enqvist and M. S. Sloth, Nucl. Phys. B **626**, 395 (2002) [arXiv:hep-ph/0109214].
D. H. Lyth and D. Wands, Phys. Lett. B **524**, 5 (2002) [arXiv:hep-ph/0110002].
T. Moroi and T. Takahashi, Phys. Lett. B **522**, 215 (2001) [Erratum-ibid. B **539**, 303 (2002)] [arXiv:hep-ph/0110096].

[6] P. Chingangbam and Q. G. Huang, arXiv:1006.4006 [astro-ph.CO].
P. Chingangbam and Q. G. Huang, JCAP **0904**, 031 (2009) [arXiv:0902.2619 [astro-ph.CO]].
Q. G. Huang and Y. Wang, JCAP **0809**, 025 (2008) [arXiv:0808.1168 [hep-th]].
Q. G. Huang, Phys. Rev. D **78**, 043515 (2008) [arXiv:0807.0050 [hep-th]].
Q. G. Huang, Phys. Lett. B **669**, 260 (2008) [arXiv:0801.0467 [hep-th]].

[7] Y. F. Cai and Y. Wang, arXiv:1005.0127 [hep-th].
J. Zhang, Y. F. Cai and Y. S. Piao, JCAP **1005**, 001 (2010) [arXiv:0912.0791 [hep-th]].
S. Li, Y. F. Cai and Y. S. Piao, Phys. Lett. B **671**, 423 (2009) [arXiv:0806.2363 [hep-ph]].
C. Lin and Y. Wang, JCAP **1007**, 011 (2010) [arXiv:1004.0461 [astro-ph.CO]].
J. O. Gong, C. Lin and Y. Wang, JCAP **1003**, 004 (2010) [arXiv:0912.2796 [astro-ph.CO]].

[8] C. T. Byrnes, K. Enqvist and T. Takahashi, arXiv:1007.5148 [astro-ph.CO].
K. Enqvist, A. Mazumdar and O. Taanila, arXiv:1007.0657 [astro-ph.CO].
L. Alabidi, K. A. Malik, C. T. Byrnes and K. Y. Choi, arXiv:1002.1700 [astro-ph.CO].
A. Mazumdar and J. Rocher, arXiv:1001.0993 [hep-ph].
S. del Campo, R. Herrera, J. Saavedra, C. Campuzano and E. Rojas, Phys. Rev. D **80**, 123531 (2009) [arXiv:0912.4721 [astro-ph.CO]].
K. Enqvist, S. Nurmi, O. Taanila and T. Takahashi, JCAP **1004**, 009 (2010) [arXiv:0912.4657 [astro-ph.CO]].
J. Sainio and I. Vilja, Phys. Rev. D **81**, 083516 (2010) [arXiv:0912.3394 [astro-ph.CO]].
C. M. Lin and K. Cheung, arXiv:0911.4749 [hep-ph].
K. Nakayama and J. Yokoyama, JCAP **1001**, 010 (2010) [arXiv:0910.0715 [astro-ph.CO]].
K. Enqvist and T. Takahashi, JCAP **0912**, 001 (2009) [arXiv:0909.5362 [astro-ph.CO]].
A. Chambers, S. Nurmi and A. Rajantie, JCAP **1001**, 012 (2010) [arXiv:0909.4535 [astro-ph.CO]].
K. Dimopoulos, M. Karciauskas and J. M. Wagstaff, Phys. Lett. B **683**, 298 (2010) [arXiv:0909.0475 [hep-ph]].
K. Dimopoulos, M. Karciauskas and J. M. Wagstaff, Phys. Rev. D **81**, 023522 (2010) [arXiv:0907.1838 [hep-ph]].

K. Enqvist, S. Nurmi, G. Rigopoulos, O. Taanila and T. Takahashi, JCAP **0911**, 003 (2009) [arXiv:0906.3126 [astro-ph.CO]].
C. M. Lin and K. Cheung, JCAP **0906**, 006 (2009) [arXiv:0904.2826 [hep-ph]].
[9] D. N. Spergel *et al.* [WMAP Collaboration], Astrophys. J. Suppl. **170**, 377 (2007) [arXiv:astro-ph/0603449].
[10] E. Komatsu *et al.* [WMAP Collaboration], Astrophys. J. Suppl. **180**, 330 (2009) [arXiv:0803.0547 [astro-ph]].
[11] E. Komatsu *et al.*, arXiv:1001.4538 [astro-ph.CO].
[12] C. Gao, Y. Gong, X. Wang and X. Chen, arXiv:1003.6056 [astro-ph.CO].
E. A. Lim, I. Sawicki and A. Vikman, JCAP **1005**, 012 (2010) [arXiv:1003.5751 [astro-ph.CO]].
[13] A. A. Starobinsky, "Multicomponent de Sitter (Inflationary) Stages and the Generation of JETP Lett. **42**, 152 (1985) [Pisma Zh. Eksp. Teor. Fiz. **42**, 124 (1985)].
M. Sasaki and E. D. Stewart, "A General Analytic Formula For The Spectral Index Of The Density Prog. Theor. Phys. **95**, 71 (1996) [arXiv:astro-ph/9507001].
D. H. Lyth and Y. Rodriguez, Phys. Rev. Lett. **95**, 121302 (2005) [arXiv:astro-ph/0504045].
[14] D. H. Lyth, K. A. Malik and M. Sasaki, JCAP **0505**, 004 (2005) [arXiv:astro-ph/0411220].
[15] M. Sasaki, J. Valiviita and D. Wands, Phys. Rev. D **74**, 103003 (2006) [arXiv:astro-ph/0607627].
[16] Q. G. Huang, JCAP **0811**, 005 (2008) [arXiv:0808.1793 [hep-th]].
[17] A. Mazumdar and J. Rocher, arXiv:1001.0993 [hep-ph].
[18] Y. F. Cai and E. N. Saridakis, arXiv:1007.3204 [astro-ph.CO].
[19] A.S.Sakharov and M.Yu.Khlopov, Yadernaya Fizika (1994) V. 57, PP. 514- 516. [English translation: Phys.Atom.Nucl. (1994) V. 57, PP. 485-487];
A.S.Sakharov, D.D.Sokoloff and M.Yu.Khlopov Yadernaya Fizika (1996) V. 59, PP. 1050-1055. [English translation: Phys.Atom.Nucl. (1996) V. 59, PP. 1005-1010];
M.Yu.Khlopov, A.S.Sakharov and D.D.Sokoloff Nucl.Phys. B (Proc. Suppl.) (1999) V. 72, 105-109;
Sergei G. Rubin, Alexander, S.Sakharov, Maxim Yu. Khlopov, J.Exp.Theor.Phys.91:921-929,2001, [hep-ph/0106187];
M.Yu. Khlopov, S.G. Rubin, A.S. Sakharov, CERN-TH-2002-033, Feb 2002.14pp. Grav. & Cosmol., v.8, Suppl. 2002, pp.57-65 [astro-ph/0202505];
Maxim.Yu. Khlopov, Sergei.G. Rubin, Alexander.S. Sakharov Astropart. Phys. (2005) V. 23, N-2, PP. 265-277. [astro-ph/0401532];
M.Yu.Khlopov, S.G.Rubin, Kluwer Academic Publishers, Dordrecht, 295 pp., 2004;
M.Yu.Khlopov, Conference series. (2007) V.66, P.012032 (10 pages). XXIX Spanish relativity meeting (ERE2006);
M.Yu.Khlopov, Res.Astron.Astrophys. (2010) V. 10, PP. 495-528, [arXiv:0801.0116].